ANTIOXIDANTS & REDOX SIGNALING
Volume 13, Number 8, 2010

DOI: 10.1089/ars.2009.3078

ORIGINAL RESEARCH COMMUNICATION

Redox Remodeling Allows and Controls B-Cell Activation and Differentiation

Roberta Vené,[1,*] Laura Delfino,[1,*] Patrizia Castellani,[1] Enrica Balza,[1] Milena Bertolotti,[2] Roberto Sitia,[2] and Anna Rubartelli[1]

Abstract

During their differentiation to antibody-secreting plasma cells, B lymphocytes undergo dramatic changes in metabolism, structure, and function. Here we show that this transition entails extensive intra- and extracellular redox changes. Lipopolysaccharide (LPS)-driven activation and differentiation of naïve murine B splenocytes is paralleled by increased production of reactive oxygen species (ROS) from different sources, followed by a strong antioxidant response. This response includes upregulation of thioredoxin and of the cystine transporter xCT, and increased production and extracellular release of nonprotein thiols, mainly glutathione (GSH) and cysteine. Although ROS levels are higher in late-differentiating B cells, an early oxidative step is likely required to start the differentiation program, because inhibition of NADPH oxidase–dependent early ROS production impairs B-cell activation and differentiation. Addition of reducing agents such as 2-ME results in increased IgM secretion per cell, suggesting that the antioxidant response not only is aimed at restoring the redox homeostasis but also plays a functional role. A highly reduced environment coincident with the presence of large ROS-producing cells is observed in histologic sections of spleens from immunized mice, indicating that the redox modifications observed in LPS-induced B-cell differentiation *in vitro* occur also *in vivo* during physiologic immune responses. *Antioxid. Redox Signal.* 13, 1145–1155.

Introduction

Proliferation and differentiation of B lymphocytes into antibody (Ab)-secreting plasma cells requires antigenic challenge and co-stimulatory signals, including signals provided by Toll-like receptors (TLRs) (34). In the mouse, B cells are more sensitive to stimulation than they are in humans, as murine B lymphocytes respond to TLR agonists such as LPS *in vitro* despite the absence of BCR activation (12).

On activation, B cells undergo profound modifications in gene and protein expression necessary to assist the massive immunoglobulin (Ig) production that will take place in plasma cells (9). In a B-cell lymphoma model, the first proteins upregulated during differentiation *in vitro* are mitochondrial and cytosolic chaperones, followed by metabolic enzymes, required to sustain energy and protein production. Endoplasmic reticulum resident proteins and proteins involved in the redox balance, such as peroxiredoxins and glutathione *S*-transferase, linearly expand during differentiation (42).

In vivo, B-cell differentiation to plasma cells takes place in the germinal centers of lymphoid organs (21) and is paralleled by strong upregulation of antioxidant systems (7). Remarkably, a hallmark of immunized lymph nodes is the massive production of nonprotein thiols (NPSH) that permeate the lymphoid tissues (7). A number of hemopoietic cells, including dendritic cells (DCs) (2), activated B cells (7), and monocytes (38) have been reported to generate low-molecular-weight thiols *in vitro*. The mechanism underlying thiol release has been recently described in lymphoma cells and called the "cystine/cysteine redox cycle" (3). This cycle involves (a) expression of xCT, the functional subunit of the Xc-transporter (36); (b) uptake of cystine, the oxidized form of the amino acid cysteine that prevails extracellularly (24); (c) intracellular conversion to reduced cysteine (2, 38); and (d) secretion of cysteine with consequent reduction of the extracellular medium (3, 8, 38).

Typically, upregulation of antioxidant systems represents a defense mechanism against oxidative stress (6). A definite analysis of the oxidative hits occurring along the differentiation process of B cells is so far missing. In principle, ROS production in activated B cells may occur through various sources. First, ROS can be produced by NADPH oxidase,

[1]National Cancer Research Institute, Genova, Italy.
[2]Division of Genetics and Cell Biology, Università Vita-Salute-San Raffaele Scientific Institute, Milano, Italy.
*These authors contributed equally to this work.

activated by BCR (31) or TLR (29) triggering. ROS might also be generated by the process of oxidative folding (see 25 and references therein). Because Ig molecules are rich in disulfide bonds, this process could result in the production of large amounts of ROS (16). Furthermore, the higher metabolic requirements in plasma cells may cause a corresponding increase in mitochondrial ROS generation. Other enzymatic sources of ROS may include P450 isoenzymes (44) or lipoxygenase (17).

ROS were originally considered only a waste product of cell metabolism that can have dangerous effects. However, compelling evidence showed that ROS are crucial intracellular signaling molecules (14). Similarly, enzymatic or nonenzymatic antioxidant systems, upregulated to counteract ROS, may have a role in signaling (32). For example, the oxidoreductase thioredoxin Trx (22) regulates a number of transcription factors in the B-cell lineage (30). The cystine/cysteine redox cycle, in addition to representing an antioxidant response to an oxidative challenge, serves a signaling function, because it concurs to promote interleukin-1β processing and secretion by LPS-stimulated monocytes (38).

In this study, we discovered the redox changes that occur along the transformation of a resting B cell to an Ab-secreting plasma cell, and investigated the relevant role of oxidative stress and of the antioxidant response in the development and outcome of B-lymphocyte differentiation. Our data indicate that ROS levels increase with differentiation and are counterbalanced by several antioxidant mechanisms. Both ROS production and the subsequent redundant antioxidant response are essential at different steps for an efficient transition of B cells to plasma cells.

Materials and Methods

Chemicals

Diphenylene iodonium (DPI), 5,5′-dithiobis-(2-nitrobenzoic acid) (DTNB), DTT, LPS, 2-ME, *N*-ethylmaleimide (NEM), cycloheximide (CHX), rotenone, metyrapone, and *nor*-dihydroguaiaretic acid, were obtained from Sigma-Aldrich. 2′,7′-Dichlorofluorescein diacetate (H_2DCF-DA), monochlorobimane (MCB), and calcein-AM were from Molecular Probes.

PeroxyGreen1 (PG1) was obtained by Dr. C.J. Chang (27).

Cell preparation and culture

BALB/c mice from Charles River (Lecco, Italy) were maintained in pathogen-free facilities. All protocols were approved by the Institutional Review Board of the Istituto Nazionale per la Ricerca sul Cancro (Genova, Italy). Spleens were removed from dead mice, and B cells were purified by positive selection on MACs columns by using anti–CD19-conjugated magnetic beads (Miltenyi Biotec), according to the manufacturer's instruction. Selected B cells were plated (1×10^6/ml) in complete RPMI supplemented with 50 μM 2-ME and activated with 20 μg/ml LPS (28, 42).

Intracellular ROS and reduced GSH detection

At each time point, cells were washed and resuspended in PBS containing 10 μM H_2DCF-DA to assess intracellular ROS (10) or 100 μM MCB, to assess intracellular GSH (11). After incubation of 20 min in the dark, cells were washed, resuspended in PBS, and FITC fluorescence (H_2DCF-DA) or Violet-1 fluorescence (MCB) was immediately measured with a flow cytometer (CyAn, Beckman Coulter) and analyzed by using Summit V4.3 software. In double-staining experiments, cells were incubated in PBS containing both fluorescent dyes. H_2DCF-DA was trapped inside cells by deesterification (40) and was also used to distinguish viable cells. To correct for any increase in fluorescence due to increased cell volume, cells were loaded in parallel with 10 μM calcein-AM and analyzed with flow cytometry (4, 18).

ELISA

IgM content in supernatants was determined with ELISA by using the Mouse IgM Quantitation Kit (Bethyl Laboratories) according to the manufacturer's instructions.

Determination of NPSH in culture media

Supernatants (0.1 ml) of murine B cells plated at 1×10^6/ml in 24-well plates in complete RPMI medium for different times were reacted with 10 mM DTNB, and the absorption was measured at 412 nm (38).

Real-time PCR

Total RNA was isolated from murine B-cells by using TriPure Isolation Reagent (Roche) and reverse-transcribed by Superscript III Reverse Transcriptase (Invitrogen), according to the manufacturer's instructions. Real-time PCR determination of cDNA was performed by using SYBR greenER qPCR Super Mix for iCycler reagent (Invitrogen). The specific primers used were forward 5′-aaacccaagtggttcagacg-3′ and reverse 5′-atctcaatcctgggcagatg-3′ (for xCT), forward 5′-atggccttccgtgttcctac-3′ and reverse 5′-gcttcaccaccttcttgatgtc-3′ (for GAPDH). Relative expression was determined by using the ΔCt method (23).

Western Blot analysis

Triton X-100 cell lysates were resolved on 12% SDS-PAGE and electrotransferred (38). Filters were probed with rabbit anti Trx (S3.1; kind gift of Dr. F. Clarke, Brisbane, Australia) and rabbit anti heme-oxygenase-1 (HO-1; Stressgen) polyclonal antibodies, or anti β-actin monoclonal Ab (Sigma-Aldrich), followed by the relevant secondary Ab (GE Healthcare), and developed with ECL-plus (GE Healthcare).

Immunization

Twelve-week-old animals (three per group) were immunized with four weekly i.p. injections of 2×10^8 sheep red blood cells (SRBC; 7). One week after the last injection, mice were killed, and the spleens removed and analyzed. All protocols were approved by the Institutional Review Board of the Istituto Nazionale per la Ricerca sul Cancro (Genova, Italy).

Staining procedures and confocal analyses

Serial cryostat sections of frozen spleens from immunized or not immunized mice were double stained with the sulfhydryl-reactive dye, Mercury Orange, as previously described (7) and with the H_2O_2-specific dye PG1 (27), or with the ROS-specific dye H_2DCF-DA (39) immediately after sectioning. Mercury Orange was incubated 5 min on ice at a

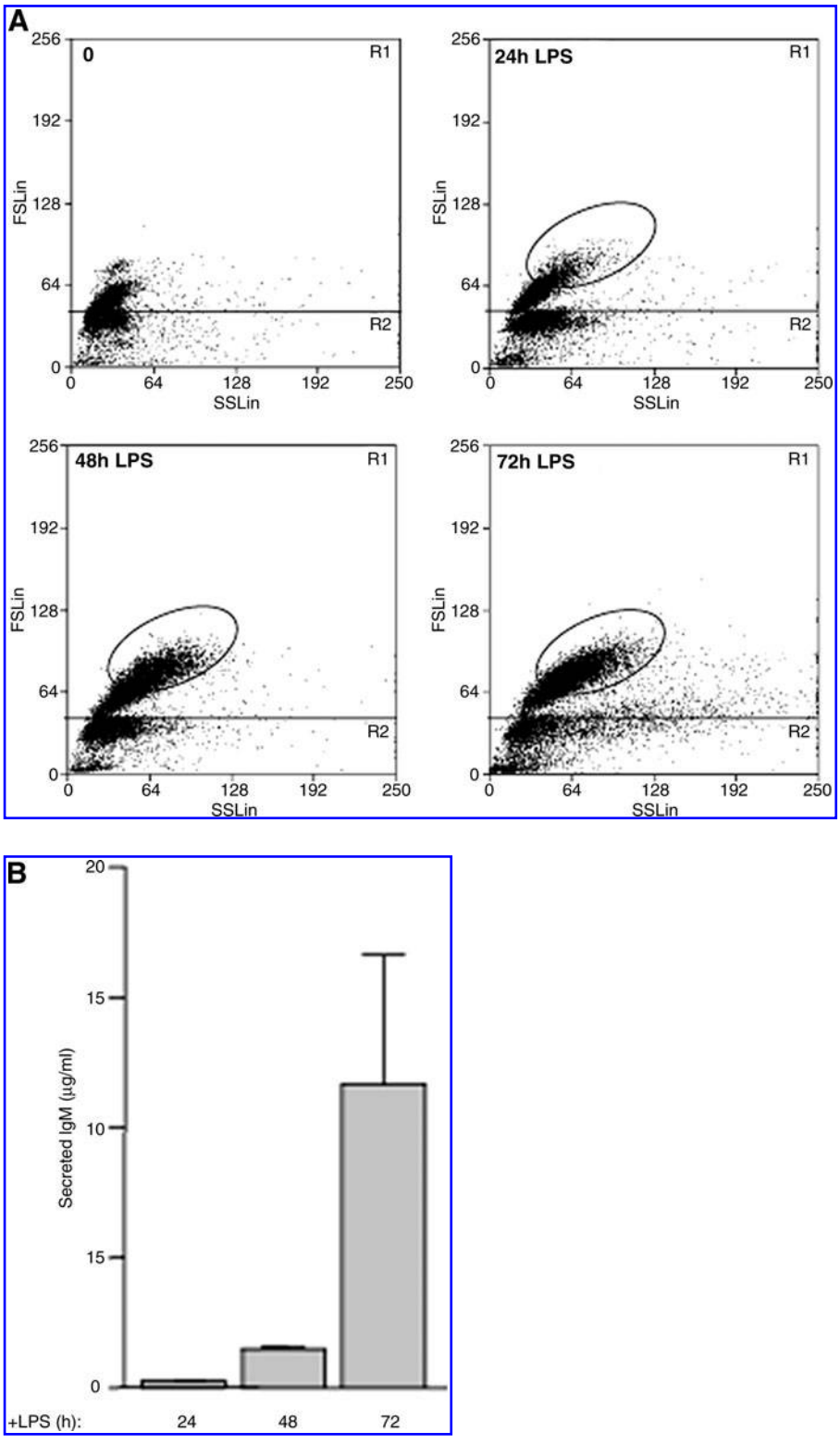

FIG. 1. LPS-induced B-lymphocyte differentiation to Ab-secreting cells. (**A**) B lymphocytes isolated from splenocytes, unstimulated or stimulated with LPS for various times, were subjected to FACS analysis. Forward (FS) and side scatter (SS) were used for preliminary identification of cells. Cells gated in R1 are viable cells. Whereas a homogeneous population of small cells is detected at time 0, a population increasing in size and complexity, corresponding to differentiating B cells, appears after 24 h from LPS stimulation and increases thereafter (*circles*). Data from one representative experiment of six performed are shown. (**B**) IgM secretion at each time point was evaluated with ELISA on supernatants. Data from three different experiments are expressed as mean micrograms IgM/ml $\pm$ SD ($p \leq 0.05$).

final concentration of 25 μM. To confirm the specificity of Mercury Orange binding to NPSH, control sections were pretreated with 100 μM NEM for 10 min to block thiol groups. Staining with PG1 (5 μM) was performed for 10 min at 37°C. Staining with H_2DCF-DA (10 μM) was performed for 30 min at 37°C. To confirm the specificity of PG1 or H_2DCF-DA staining, control sections were pretreated with 1 mM DTT for 10 min. The sections were analyzed with confocal microscopy, and the images were acquired with the Fluoview FV500 software.

For double immunofluorescence, rabbit anti-mouse Trx (S3.1), rabbit anti-HO-1 (Stressgen), rat anti-CD45R B cells (R&D), and rat anti-F4/80 tissue macrophage (19, Novus

Biologicals) antibodies were used. Rhodamine (TRITC)-labeled anti-rat IgG or FITC-labeled anti-rabbit IgG (Jackson Immunoresearch) were used as secondary Abs. Images were acquired with Leica DM LB-2 microscopy by using Scion Image software.

Statistical analysis

The data were statistically analyzed with a one-way ANOVA test, followed by Bonferroni posttest, or with an unpaired *t* test by using GraphPad software.

Results

ROS production during B cell differentiation

LPS stimulation *in vitro* of B splenocytes from naïve mice results in activation of a fraction of B cells (28). As shown in Fig. 1A, activated B lymphocytes (R1, encircled) increase in size and complexity, appearing as a rather homogeneous population of cells larger than resting B cells that emerges 24 h from LPS stimulation and increases thereafter. Nonactivated B cells remain of small dimensions and low complexity (R1, not encircled) or die (R2). Analysis of IgM secretion revealed a dramatic increase at day 3 (Fig. 1B), in agreement with the typical kinetics of secretion induced by LPS *in vitro* (42).

To assess ROS production, resting B splenocytes were exposed to H_2DCF-DA at various times from LPS stimulation. As shown in Fig. 2A, ROS were only slightly increased in the first 2 h of exposure to the mitogen. A significant enhancement in ROS levels was detected after 24 h of culture and increased along with B-cell differentiation. Although all living cells stained with the vital dye H_2DCF-DA (Fig. 2B, R2 and R4), small cells (Fig. 2B, R4) were less positive, and the highest levels of ROS were found in the large, differentiating B cells (Fig. 2B, R2). To correct for the fluorescence increase merely due to enlarged cell volume, B cells were loaded in parallel with the vital dye calcein-AM (4, 18), and the H_2DCF-DA fluorescence increase at each time point was normalized versus the increase in calcein-AM (Fig. 2C). The results confirmed that the increment of H_2DCF-DA fluorescence is due to

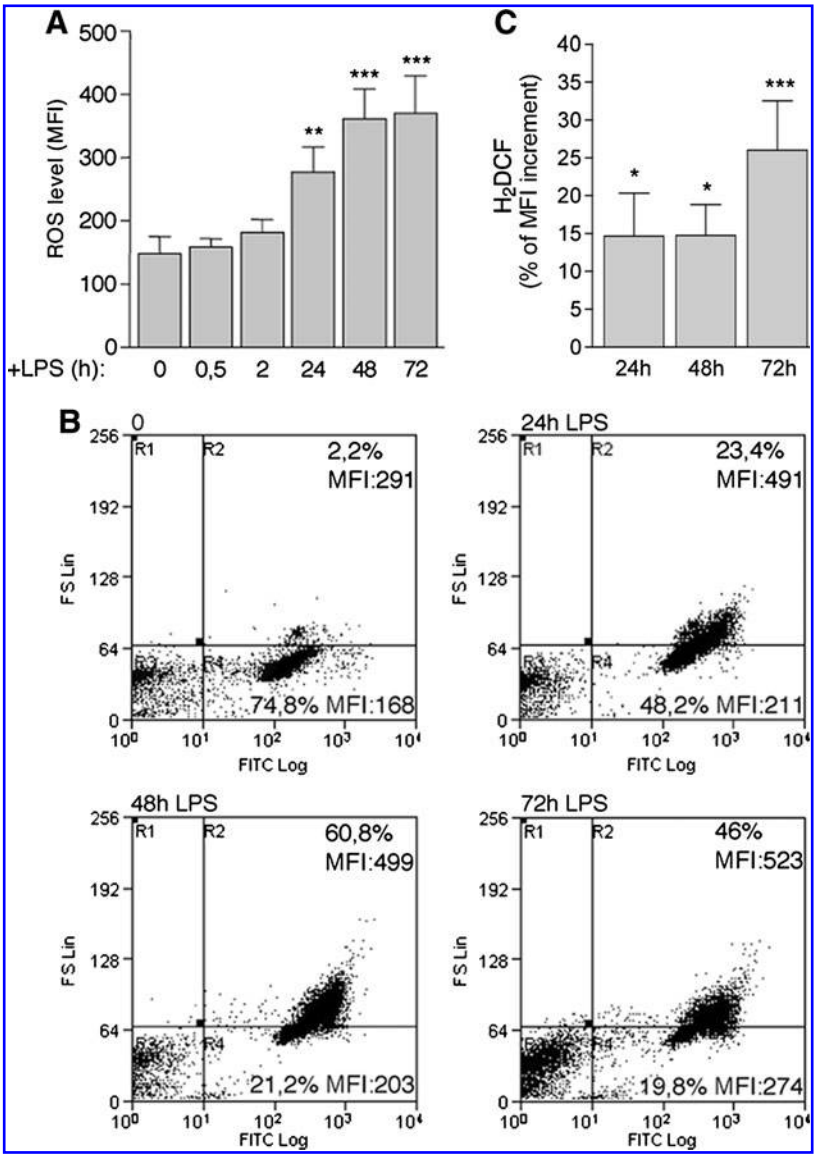

FIG. 2. LPS-induced B-lymphocyte differentiation is accompanied by increased ROS production. B splenocytes at different times from exposure to LPS, as indicated, were loaded with H_2DCF-DA or calcein-AM and analyzed with FACS. (**A**) Data are expressed as mean fluorescence intensity (MFI) in all living cells ± SD. $^{***}p \leq 0.001$; $^{**}p \leq 0.01$. (**B**) Cells were gated according to size and fluorescence. R2 includes large differentiating B cells; R4 includes small, living B cells; R3 includes dead cells and debris. Results are expressed as percentage of positive cells and MFI. (**C**) H_2DCF-DA staining increase at each time point compared with time 0 was subtracted from the increase in calcein-AM fluorescence, according to the formula: increment of H_2DCF-DA MFI/increment of calcein-AM MFI. Data are expressed as percentage of H_2DCF-DA increment with respect to time 0. $^{*}p \leq 0.05$. Data are representative of at least three independent experiments.

increased ROS production along with B-cell differentiation (Fig. 2C and Supplemental Fig. 1; *see* www.liebertonline.com/ars).

Different mechanisms concur to ROS production

B cells at various times from LPS stimulation were treated for 3 h with compounds that inhibit ROS generation by different sources, namely DPI, which blocks NADPH oxidase (15); rotenone, which inhibits mitochondrial ROS production (13); or with the protein-synthesis inhibitor cycloheximide (CHX). At the end of the incubation, cells were loaded with H_2DCF-DA, and ROS production was assessed with FACS analysis. DPI decreased ROS generation at all times (24, 48, and 72 h from LPS stimulation), resulting in a 30–40% of inhibition with respect to control cells (Fig. 3A). Similarly, rotenone affected ROS production at all times, causing a decrease of 20–30%, whereas CHX resulted in only a slight reduction in ROS generation (Fig. 3A). Metyrapone, a potent inhibitor of cytochrome P450 (44), and *nor*-dihydroguaiaretic acid, which blocks the lipoxygenase activity (17), barely affected ROS production, even at high dosage (data not shown).

As expected, CHX treatment strongly inhibited IgM secretion (Fig. 3B). The decreased ROS production observed in 72-h LPS-stimulated B cells during 3 h of exposure to DPI and rotenone (Fig. 3A) also correlated with a decreased IgM secretion (Fig. 3B).

Activation of antioxidant responses in ROS-producing cells

Next, we examined the activation of antioxidant systems in differentiating B cells. As shown in Fig. 4, the levels of GSH, the major intracellular electron donor (26), doubled in the first 24 h of stimulation with LPS and increased thereafter (Fig. 4A and B). The highest GSH increase was observed in larger, differentiating cells (Fig. 4C, R2). Remarkably, double staining revealed that the same cells that produce more ROS also produce more GSH (Fig. 4D). Normalization versus calcein-AM staining (4, 18) at each time point confirmed that the strong enhancement in MCB fluorescence was actually due to a dramatic increase in GSH, more evident at 48 h from stimulation (Fig. 4E).

In addition to GSH, the cystine/cysteine redox cycle was upregulated in differentiating B cells, with a delay compared with ROS induction. Expression of xCT, very low or absent in resting B cells (7), was induced by LPS and increased along with B-cell differentiation (Fig. 5A). Likewise, extracellular cysteine accumulated significantly 48 h from exposure to LPS and increased thereafter (Fig. 5B). Intracellular Trx was also strongly increased in differentiating B lymphocytes (Fig. 5C), with kinetics that paralleled cysteine release (panel B). The oxidant-responsive enzyme HO-1 (34) was upregulated in LPS-stimulated B cells, and its expression was delayed compared with that of thioredoxin.

Different redox requirements in the early and late phases of terminal B-cell differentiation

NADPH-oxidase–dependent ROS generation has been proposed as a crucial event in B-cell activation (31). Our assays, however, did not reveal significant ROS increases early after LPS stimulation (from 5 min to 2 h; Fig. 2A and data not shown), possibly because of insufficient sensitivity of H_2DCF-DA or rapid ROS scavenging. To investigate further the potential signaling role of ROS in the early activation phases, B cells were exposed to LPS in the presence of DPI, to block NADPH-oxidase–dependent ROS production. DPI was highly toxic for freshly isolated resting B cells that died at DPI doses not affecting the viability of different white blood cells (38; data not shown). Therefore, lower concentrations (100 and 200 n*M*) were used to limit cytotoxicity. DPI-treated B cells displayed a mild decrease in ROS levels both at 24 and

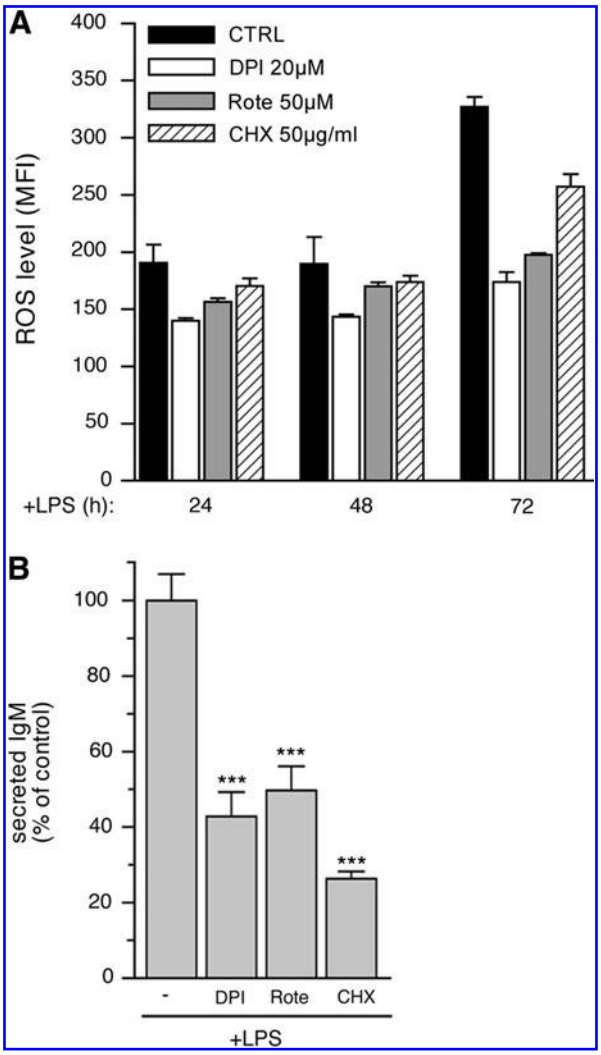

FIG. 3. Effect of DPI, rotenone, and CHX on ROS production and IgM secretion. (**A**) B cells at 24, 48, or 72 h from LPS stimulation were resuspended in fresh medium and incubated 3 h in the presence or absence of DPI, rotenone (rote), or CHX. At the end of the incubation, ROS analysis was performed, as in Fig. 2. Results are expressed as MFI in living cells ± SD. Data from a representative experiment of three performed are shown. (**B**) IgM secretion was quantified with ELISA in supernatants of 72-h LPS-stimulated B cells incubated 3 h in fresh medium in the presence or absence of DPI, rotenone (rote), or CHX, as in (**A**). Results are expressed as percentage of IgM secreted by control cells stimulated with LPS in the absence of inhibitors ± SD (***$p \leq 0.001$). Data from a representative experiment, carried out in triplicate, of two performed, are shown.

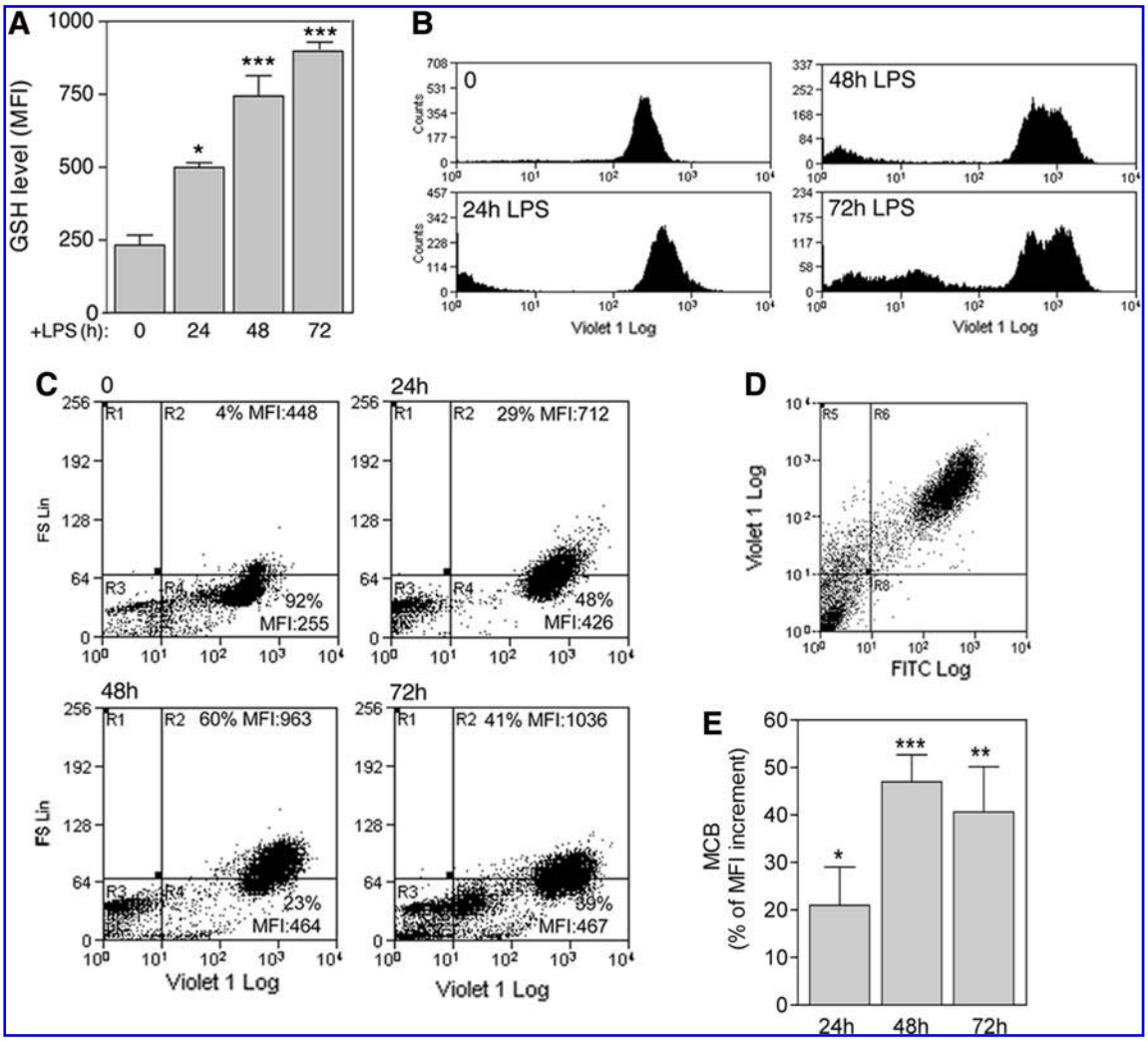

FIG. 4. Intracellular reduced GSH increases in differentiating B cells. (**A**) MCB staining of reduced GSH in B splenocytes at different times from exposure to LPS. Data are expressed as MFI in all living cells ± SD (mean of two independent experiments). ***$p \leq 0.001$; *$p \leq 0.05$. (**B**) Peaks of MCB fluorescence intensity in LPS-treated cells at days 0, 1, 2, and 3. (**C**) MCB staining expressed as percentage of positive cells and MFI in B-cell populations gated as in Fig. 2B. (**D**) Double staining with H_2DCF-DA and MCB in living cells at 72 h after LPS stimulation. Data are representative of at least three independent experiments. (**E**) MCB staining increase was normalized versus the increase in calcein-AM fluorescence, as in Fig. 2C. Data are expressed as percentage of MCB increment versus time 0, subtracted from calcein-AM increment. ***$p \leq 0.001$; **$p \leq 0.01$; *$p \leq 0.05$.

48 h (Fig. 6A). Moreover, the amount of secreted IgM, normalized on a "per viable cell" basis, was reduced in DPI-treated B-cell culture (Fig. 6B).

Exposure to DPI also resulted in a decreased cysteine release by LPS-treated B lymphocytes (Fig. 6C), supporting the hypothesis that the upregulation of antioxidant systems occurring in differentiating B lymphocytes represents a response to an LPS-induced oxidative hit. To assess whether the antioxidant response affects differentiation, B lymphocytes were stimulated with LPS in the presence of 0.8 m*M* 2-ME. Under these conditions, the percentage of cells dying at 24 h of culture shows increases of 15–25% in the different experiments (data not shown), so that the number of differentiating B cells is smaller. However, Ab-secreting cells generated in the presence of 2-ME displayed a higher IgM secretion rate than did controls (Fig. 6B).

Oxidative and reducing events in B cell follicles of naïve or immunized spleen

To investigate the sites of ROS and NPSH accumulation in lymphoid organs *in vivo*, spleens from naïve or SRBC-immunized mice were stained with H_2DCF-DA (that reacts mainly with H_2O_2 and peroxynitrite), PG1 (which specifically stains H_2O_2), or with the free thiol-binding dye Mercury Orange. Nonimmunized spleens did not stain with PG1 (Fig. 7A) or H_2DCF-DA (not shown), and displayed a weak staining with Mercury Orange (Fig. 7A). In contrast, spleens from immunized animals showed a diffuse staining with PG1 (Fig. 7B) or with H_2DCF-DA (Fig. 7C), which was stronger in clusters of cells within germinal centers (Fig. 7G). Remarkably, cells highly stained with the ROS probes were also the most positive to Mercury Orange (Fig. 7B and C). The

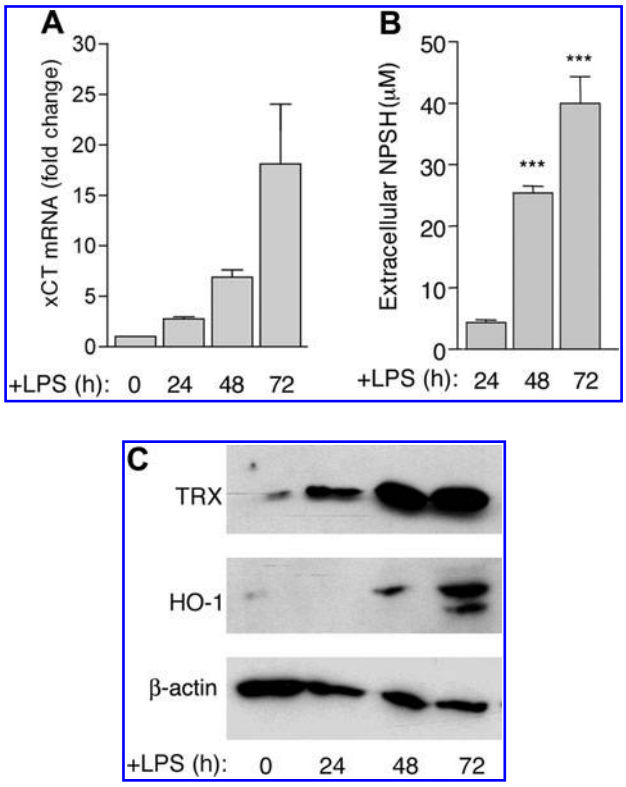

FIG. 5. Induction of antioxidant enzymes and of NPSH extracellular release along with B-lymphocyte differentiation. (**A**) xCT mRNA relative expression was evaluated with real-time PCR at different times. Data are expressed as fold change at 24, 48, and 72 h from LPS stimulation with respect to day 0 ($p \leq 0.05$). (**B**) NPSH levels in cell supernatant at 24, 48, and 72 h after LPS stimulation. Data are expressed as micromolar concentration of released NPSH (mean of triplicate ± SD). (**C**) Western blot analysis of TRX (**upper panel**) and HO-1 (**middle panel**) proteins on cell lysates from unstimulated (0), or 24, 48, and 72 h LPS-treated cells. The **lower panel** shows the same blot hybridized with anti-actin, as a loading control. Data are representative of at least three independent experiments.

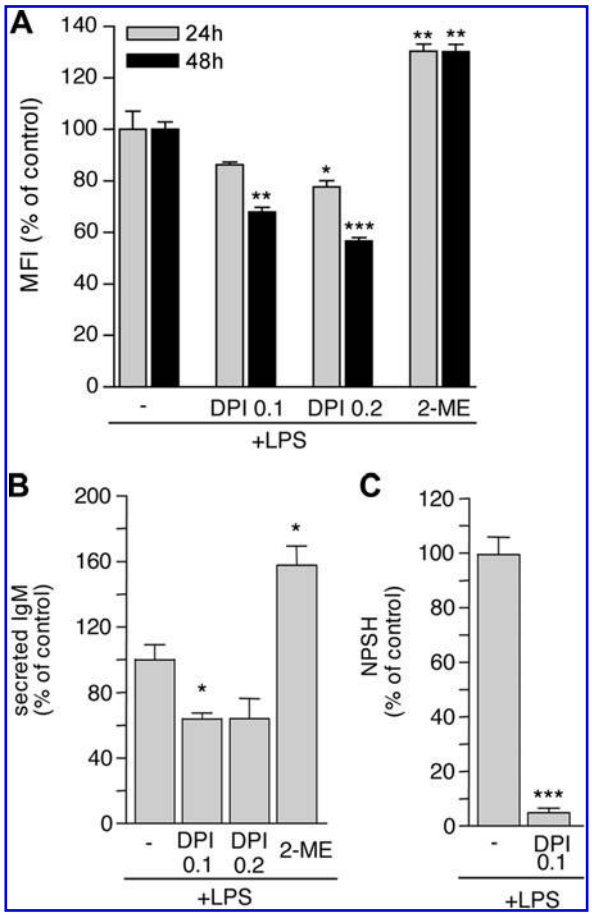

FIG. 6. The presence of DPI or 2-ME impairs LPS-driven B-cell differentiation. **(A)** B cells were exposed to LPS in the presence or absence of 0.1 or 0.2 μM DPI or 800 μM 2-ME. After 24 h (light columns) or 48 h, cells (dark columns) were loaded with H_2DCF-DA and subjected to FACS analysis. Data are expressed as percentage of MFI of LPS-treated control cells. (**B**) IgM secretion at 48 h was evaluated with ELISA. Data were normalized to the number of living cells evaluated with Trypan Blue exclusion staining and are expressed as percentage of IgM secreted by LPS-treated control cells. (**C**) Cysteine release by cells stimulated with LPS for 48 h in the presence of 100 nM DPI. Data are expressed as percentage of release by control cells, stimulated without DPI. Mean of at least two different experiments ± SD is shown. *$p \leq 0.05$; **$p \leq 0.01$; ***$p \leq 0.001$.

specificity of the ROS and NPSH staining was confirmed by the control experiments shown in Fig. 7D–F. ROS staining by PG1 and H_2DCF-DA was prevented by incubating spleen sections with the reducing agent DTT (Fig. 7D and E), whereas Mercury Orange staining was prevented by treatment of spleen sections with NEM, which blocks free thiols (Fig. 7F).

Spleen sections from nonimmunized (Fig. 8A and B) and immunized (Fig. 8C–E) mice were then analyzed with double immunofluorescence with anti-Trx (Fig. 8A and C) or anti-HO-1 (Fig. 8B, D, and E) and CD45R (Fig. 8A–D) or F480 (Fig. 8E) antibodies. A mild positivity for Trx was found in nonimmunized spleens, restricted to the interfollicular areas, but absent from the B-cell follicle (Fig. 8A). In immunized spleens, Trx staining was increased in the interfollicular areas and was clearly strongly detected also in groups of differentiating B cells within the germinal centers (Fig. 8C). Trx staining appeared slightly diffuse, probably because of its secretion and extracellular diffusion (33). HO-1 was mildly detected in the interfollicular areas of nonimmunized spleens (Fig. 8B), whereas it was strongly positive both in interfollicular cells and in a few germinal-center B cells (Fig. 8D). Interfollicular HO-1–positive cells were not stained by markers of B cells, T cells, granulocytes, DCs, and macrophages of the T-cell areas (not shown) but were strongly positive for the red pulp macrophage marker F4/80 (Fig. 8E).

Discussion

We followed the oxidant and antioxidant events occurring in B lymphocytes during their transition to plasma cells and found that ROS generation accompanies the differentiation process and is counterbalanced by a strong upregulation of antioxidant defense mechanisms.

The increase in ROS, detected since 24 h from LPS stimulation, was hindered by inhibitors of protein synthesis and of

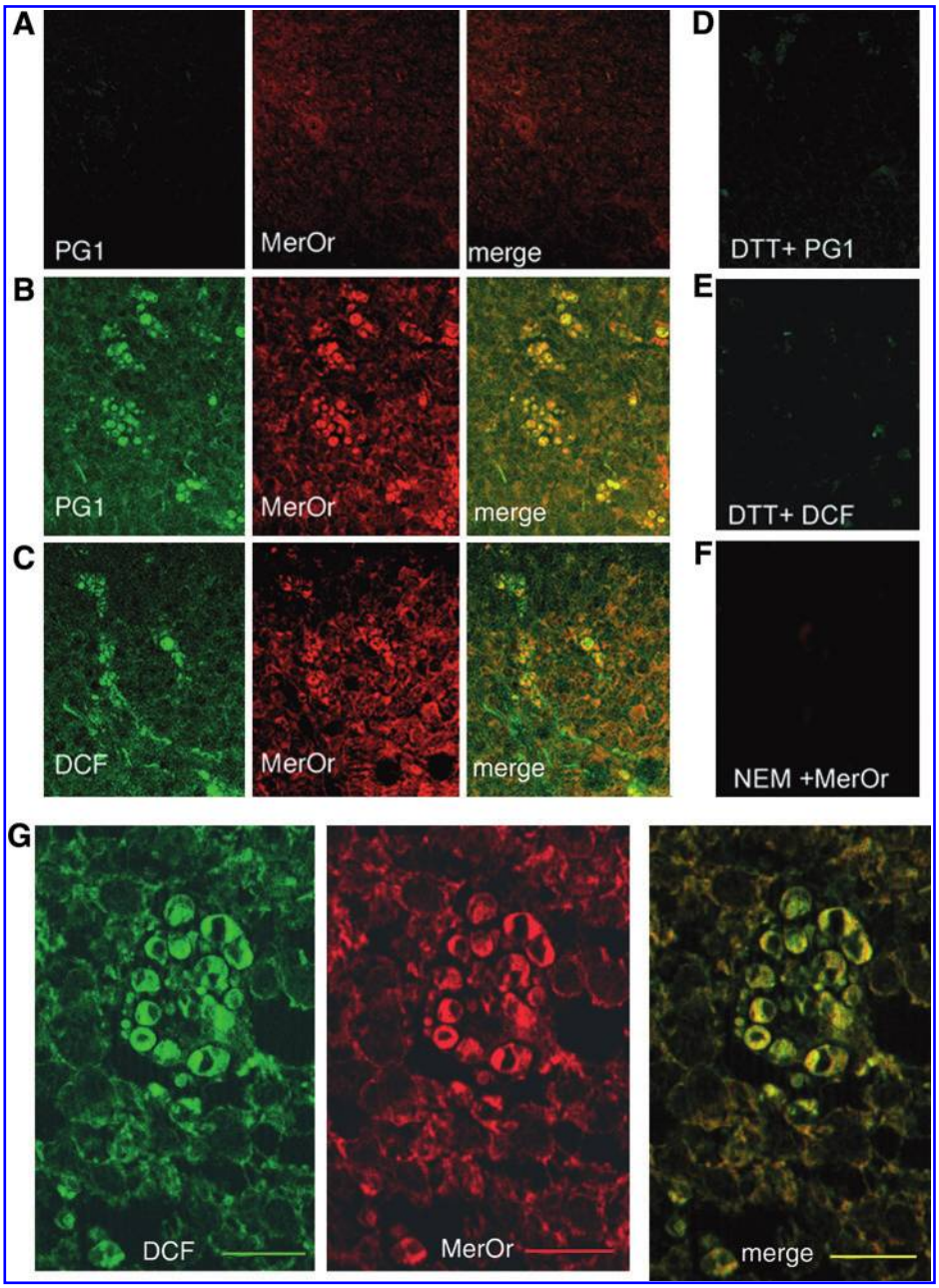

FIG. 7. ROS and NPSH staining cluster in germinal center of immunized spleens. Spleens were removed from non-immunized mice (**A**) or from mice immunized with SRBC, 1 week after the last injection (**B**, **C**). Spleen sections were double stained with PG1 and Mercury Orange (MerOr) (**A**, **B**) or H_2DCF-DA (DCF) and Mercury Orange (MerOr) (**C, G**) and analyzed with confocal microscopy. (**D**, **E**) PG1 and CH_2DCF-DA staining were prevented by neutralization of ROS by pre-incubation of spleen sections with 1 m*M* DTT for 10 min. (**F**) Mercury Orange staining was prevented by blocking thiol groups with 100 μM NEM for 10 min. Magnification 60×(**A–F**); 100×(**G**). (For interpretation of the references to color in this figure legend, the reader is referred to the web version of this article at www.liebertonline.com/ars).

different ROS-generating systems, including NADPH oxidases and the mitochondrial electron-transport chain. The degree of inhibition observed at all times with the single drugs ranged between 15% (with CHX) and 35% (with DPI or rotenone), indicating that ROS are simultaneously produced by different intracellular sources throughout differentiation. In addition, the modest decrease in ROS levels induced by CHX suggests that neither the high rates of Ig biosynthesis nor the process of Ig oxidative folding is responsible for the strong ROS increase. Rather, the observation that ROS are generated at high levels even when Ig production is blocked is in agreement with previous findings that, on activation, B cells expand their metabolic capacity and secretory machinery well before IgM secretion starts (42). The increased energetic metabolism and the massive expansion of the secretory apparatus may account *per se* for ROS production.

ROS increase is followed by upregulation of various antioxidant systems (6). We focused on three of these systems, different although related: intracellular glutathione, antioxidant enzymes (Trx and HO-1), and the cystine/cysteine redox cycle. Glutathione, the principal redox buffering system in living cells (26), seems to act as a first line of defense against oxidative stress in LPS-activated B lymphocytes, because it increases early, almost simultaneous with ROS. The increase of the key redox-regulating protein Trx (22) is dramatic but delayed with respect to GSH, confirming also in primary B lymphocytes the observation that Trx levels are lower in B-cell than in plasmacytic tumor cell lines (30). The increased expression of the HO-1 (35) late along the differentiation process of B cells is a novel finding. Indeed, although HO-1 is emerging as a key regulator of T cell–mediated immunity (43), no data on expression or function in B cells have been re-

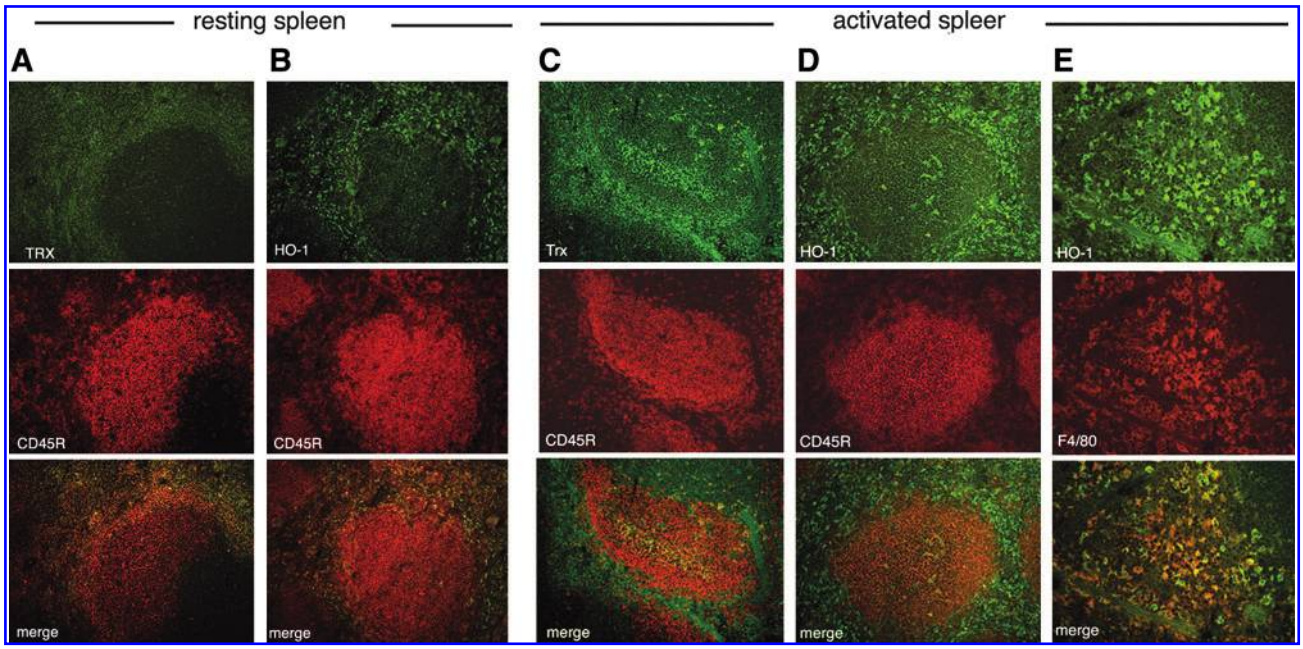

FIG. 8. TRX and HO-1 spleen expression and localization in immunized spleen. Double immunofluorescence analysis of spleen sections from nonimmunized (**A, B**) or immunized (**C–E**) mice with anti-CD45R and anti-Trx Ab (**A** and **C**), anti-CD45R and anti-HO1 Ab (**B** and **D**), anti-HO1 and anti F4/80 Ab (**E**). Magnification: 20×(**A–D**) and 40×(**E**). (For interpretation of the references to color in this figure legend, the reader is referred to the web version of this article at www.liebertonline.com/ars).

ported. Because this enzyme has been proposed as an anti-apoptotic factor (5, 37), its expression could be finalized to delay in the death of antibody-secreting cells.

In addition to GSH and oxido-reductases, we identified a third antioxidant system upregulated in differentiating B lymphocytes, the cystine/cysteine redox cycle. The increase in this cycle is a key event in T-cell activation by antigen-presenting DCs (2) and IL-1β secretion by monocytes (38). Its importance in redox homeostasis was recently highlighted also in tumors (3, 8).

Our data show that blocking NADPH-oxidase–dependent ROS production with DPI impairs B-cell activation/differentiation as well as the efficiency of IgM secretion. This result is in line with the previous suggestion (31) that H_2O_2 may act as a secondary messenger in the initiation and amplification of signaling after BCR triggering. However, we failed to detect ROS increase in the first hours after LPS stimulation. This is possibly due to a low increase of ROS over basal levels, undetectable by standard methods, or to a too-rapid ROS scavenging in this phase. An alternative explanation is that other cells, such as monocytes or granulocytes, that undergo an oxidative burst on activation, provide ROS for activating the neighboring lymphocytes (31). In our culture conditions, however, granulocytes were virtually absent, and macrophages consistently were <1% (not shown). Moreover, LPS stimulation in the presence of splenic macrophages increased neither the number of B cells entering the differentiation program nor the efficiency of IgM secretion (not shown).

A novel finding of this study is that not only the oxidative burst but also the antioxidant responses are implicated in the differentiation of B lymphocytes. When the reducing agent 2-ME is added to resting B cells at the beginning of the culture, the number of B cells that survive and differentiate to LPS is severely reduced, suggesting that highly reducing conditions are detrimental in the early phases of B-cell activation.

Conversely, the rate of IgM secretion per cell is increased in the presence of 2-ME, indicating that, later on during differentiation, reduction of the microenvironment promotes IgM secretion. This effect is likely due to the facilitated transport of Ig-assembly intermediates along the exocytoxic pathway. It was previously observed that the addition of reducing agents to the culture medium, at concentrations that do not affect cell viability and do not cause disassembly of IgM monomers or unfolding of individual Ig chains, allows secretion of unpolymerized IgM otherwise retained in the ER by disulfide-interchange reactions (1, 41).

In vitro experimental systems of B-cell activation and differentiation provide many advantages, including the possibility for study of purified cell populations and the determination of the kinetics of the events that follow LPS stimulation. However, many factors may alter the correct development of the Ab response *in vitro*, such as the unavoidable cell manipulations that stress the cells and may change their redox, and the high oxygen tension that can impair significantly the redox regulation. Furthermore, the redox changes observed *in vitro* may be restricted to the B-cell population responsive to TLR4 triggering. To circumvent these constraints, we studied spleens from nonimmunized or SRBC-immunized animals. These experiments demonstrated that a dramatic redox reshaping during B-cell differentiation occurs also in response to a specific antigen in the complex choreography of the immune response *in vivo*. Confocal fluorescence analyses revealed that a minority of B cells in the germinal center produce high levels of ROS, and in all cases, these cells also increased levels of NPSH, thereby confirming the co-staining of ROS and GSH observed in differentiating B

cells *in vitro*. The finding that the same cells concomitantly stain with reagents specific for ROS and antioxidants is only apparently discrepant. In a given cell, as long as the oxidative stress persists, antioxidant responses must continue. Moreover, NPSH, revealed by Mercury Orange, may not neutralize ROS directly but rather may protect targets of ROS from oxidation. Support for this interpretation comes from the *in vitro* finding that ROS detection is not impaired in the presence of 2-ME.

Interestingly, in addition to the few B cells highly reacting to the dyes specific for ROS and NPSH, all germinal centers were diffusely stained. This observation suggests that ROS and NPSH are not confined within the producing cells but are released in the microenvironment, where they diffuse and generate redox gradients. NPSH is actively secreted by differentiating B lymphocytes through the cystine/cysteine cycle, and ROS can be generated extracellularly by NADPH oxidases and perhaps secreted as well.

In vitro, differentiated B lymphocytes express high levels of TRX and HO-1. Interestingly, in immunized spleen sections, these enzymes are highly expressed, not only in B cells in the germinal centers, but also in red-pulp macrophages. This finding suggests that antioxidant enzymes, besides affording cytoprotection against oxidative injury (20), may represent a barrier to segregate B follicles from each other, preserving the intrafollicular redox from external stress. In the first phases of the soluble immune response, when Ag-specific B cells are triggered, resulting in oxidative stress within the developing germinal center, HO-1 and Trx may block the diffusion of ROS to other follicles. This fence may prevent premature redox responses in other follicles that could impede correct B-cell activation, in keeping with the *in vitro* observation that the presence of 2-ME reduces the number of B cells that survive and differentiate in response to LPS.

In conclusion, we showed that intra- and intercellular redox remodeling occurs during terminal B-cell differentiation. We propose that ROS production and the consequent antioxidant responses serve signaling and homeostatic functions necessary for full-fledged plasma cell differentiation.

Acknowledgments

We thank Dr. P. Castagnola for help with confocal analyses, Dr. F. Clarke for the generous gift of anti TRX, and Dr. C.J. Chang for kindly providing PeroxyGreen 1. This work was supported in part by grants from Ministero della Salute, Ministero Università e Ricerca, ISS, Cariplo, Compagnia di San Paolo, Telethon.

Author Disclosure Statement

No competing financial interests exist

References

1. Alberini CM, Bet P, Milstein C, and Sitia R. Secretion of immunoglobulin M assembly intermediates in the presence of reducing agents. *Nature* 347: 485–487, 1990.
2. Angelini G, Gardella S, Ardy M, Ciriolo MR, Filomeni G, Di Trapani G, Clarke F, Sitia R, and Rubartelli A. Antigen-presenting dendritic cells provide the reducing extracellular microenvironment required for T lymphocyte activation. *Proc Natl Acad Sci U S A* 99: 1491–1496, 2002.
3. Banjac A, Perisic T, Sato H, Seiler A, Bannai S, Weiss N, Kölle P, Tschoep K, Issels RD, Daniel PT, Conrad M, and Bornkamm GW. The cystine/cysteine cycle: a redox cycle regulating susceptibility versus resistance to cell death. *Oncogene* 27: 1618–1628, 2008.
4. Braut-Boucher F, Pichon J, Rat P, Adolphe M, Aubery M, and Font J. A non-isotopic, highly sensitive, fluorimetric, cell-cell adhesion microplate assay using calcein AM-labeled lymphocytes. *J Immunol Methods* 178: 41–51, 1995.
5. Brouard S, Otterbein LE, Anrather J, Tobiasch E, Bach FH, Choi AM, and Soares MP. Carbon monoxide generated by heme oxygenase 1 suppresses endothelial cell apoptosis. *J Exp Med* 192: 1015–1025, 2000.
6. Carta S, Castellani P, Delfino L, Tassi S, Venè R, and Rubartelli A. DAMPs and inflammatory processes: the role of redox in the different outcomes. *J Leukoc Biol* 86: 549–555, 2009.
7. Castellani P, Angelini G, Delfino L, Matucci A, and Rubartelli A. The thiol redox state of lymphoid organs is modified by immunization: role of different immune cell populations. *Eur J Immunol* 38: 2419–2425, 2008.
8. Ceccarelli J, Delfino L, Zappia E, Castellani P, Borghi M, Ferrini S, Tosetti F, and Rubartelli A. The redox state of the lung cancer microenvironment depends on the levels of thioredoxin expressed by tumor cells and affects tumor progression and response to prooxidants. *Int J Cancer* 123: 1770–1778, 2008.
9. Cenci S and Sitia R. Managing and exploiting stress in the antibody factory. *FEBS Lett* 581: 3652–3657, 2007.
10. Chandra J, Tracy J, Loegering D, Flatten K, Verstovsek S, Beran M, Gorre M, Estrov Z, Donato N, Talpaz M, Sawyers C, Bhalla K, Karp J, Sausville E, and Kaufmann SH. Adaphostin-induced oxidative stress overcomes BCR/ABL mutation-dependent and -independent imatinib resistance. *Blood* 107: 2501–2506, 2006.
11. Chen WY, Chang FR, Huang ZY, Chen JH, Wu YC, and Wu CC. Tubocapsenolide A, a novel withanolide, inhibits proliferation and induces apoptosis in MDA-MB-231 cells by thiol oxidation of heat shock proteins. *J Biol Chem* 283: 17184–17193, 2008.
12. Coutinho A, Gronowicz E, Bullock WW, and Moller G. Mechanism of thymus-independent immunocyte triggering: mitogenic activation of B cells results in specific immune responses. *J Exp Med* 139: 74–92, 1974.
13. Del Prete A, Zaccagnino P, Di Paola M, Saltarella M, Oliveros Celis C, Nico B, Santoro G, and Lorusso M. Role of mitochondria and reactive oxygen species in dendritic cell differentiation and functions. *Free Radic Biol Med* 44: 1443–1451, 2008.
14. Droge W. Free radicals in the physiological control of cell function. *Physiol Rev* 82: 47–95, 2002.
15. Ellis JA, Mayer SJ, and Jones OT. The effect of the NADPH oxidase inhibitor diphenyleneiodonium on aerobic and anaerobic microbicidal activities of human neutrophils. *Biochem J* 251: 887–891, 1988
16. Enyedi B, Várnai P, and Geiszt M. Redox state of the endoplasmic reticulum is controlled by *Ero*1L-alpha and intraluminal calcium. *Antioxid Redox Signal* 13: 721–729, 2010.
17. Fedyk ER and Phipps RP. Reactive oxygen species and not lipoxygenase products are required for mouse B-lymphocyte activation and differentiation. *Int J Immunopharmacol* 16: 533–546, 1994.

18. Hamann S, Kiilgaard JF, Litman T, Alvarez-Leefmans FG, Winther BR, and Zeuthen T. Measurement of cell volume changes by fluorescence self-quenching. *J Fluoresc* 12: 139–145, 2002.
19. Hume DA, Robinson AP, MacPherson GG, and Gordon S. The mononuclear phagocyte system of the mouse defined by immunohistochemical localization of antigen F4/80: relationship between macrophages, Langerhans cells, reticular cells, and dendritic cells in lymphoid and hematopoietic organs. *J Exp Med* 158: 1522–1536, 1983.
20. Kensler TW, Wakabayashi N, and Biswal S. Cell survival responses to environmental stresses via the Keap1-Nrf2-ARE pathway. *Annu Rev Pharmacol Toxicol* 47: 89–116, 2007.
21. Klein U and Dalla-Favera R. Germinal centres: role in B cell physiology and malignancy. *Nat Rev Immunol* 8: 22–33, 2008.
22. Lillig CH and Holmgren A. Thioredoxin and related molecules: from biology to health and disease. *Antioxid Redox Signal* 9: 25–47, 2007.
23. Livak KJ and Schmittgen TD. Analysis of relative gene expression data using real time quantitative PCR and the 2 ΔCT method. *Methods* 24: 402–408, 2001.
24. Mansoor MA, Svardal AM, and Ueland PM. Determination of the in vivo redox status of cysteine, cysteinylglycine, homocysteine, and glutathione in human plasma. *Anal Biochem* 200: 218–229, 1992.
25. Masciarelli S and Sitia R. Building and operating an antibody factory: redox control during B to plasma cell terminal differentiation. *Biochim Biophys Acta* 1783: 578–588, 2008.
26. Meister A. Glutathione metabolism. *Methods Enzymol* 251: 3–7, 1995.
27. Miller EW, Tulyathan O, Isacoff EY, and Chang CJ. Molecular imaging of hydrogen peroxide produced for cell signaling. *Nat Chem Biol* 3: 263–267, 2007.
28. Mond JJ and Brunswick M. Proliferative assays for B cell function. *Curr Protoc Immunol* Chapter 3: Unit 3–10, 2003.
29. Moon EY, Lee JH, Oh SJ, Ryu SK, Kim HM, Kwak HS, and Yoon WK. Reactive oxygen species augment B-cell-activating factor expression. *Free Radic Biol Med* 40: 2103–2111, 2006.
30. Nilsson J, Söderberg O, Nilsson K, and Rosén A. Differentiation-associated redox-regulation in human B cell lines from stem cell/pro-B to plasma cell. *Immunol Lett* 94: 83–89, 2004.
31. Reth M. Hydrogen peroxide as second messenger in lymphocyte activation. *Nat Immunol* 3: 1129–1134, 2002.
32. Rubartelli A and Sitia R. Stress as an intercellular signal: the emergence of stress-associated molecular patterns (SAMP). *Antiox Redox Signal* 11: 2621–2629, 2009.
33. Rubartelli A, Bajetto A, Allavena G, Wollman E, and Sitia R. Secretion of thioredoxin by normal and neoplastic cells through a leaderless secretory pathway. *J Biol Chem* 267: 24161–24164, 1992.
34. Ruprecht CR and Lanzavecchia A. Toll-like receptor stimulation as a third signal required for activation of human naive B cells. *Eur J Immunol* 36: 810–816, 2006.
35. Ryter SW and Choi AM. Heme oxygenase-1: redox regulation of a stress protein in lung and cell culture models. *Antioxid Redox Signal* 7: 80–91, 2005.
36. Sato H, Tamba M, Ishii T, and Bannai S. Cloning and expression of a plasma membrane cystine/glutamate exchange transporter composed of two distinct proteins. *J Biol Chem* 274: 11455–11458, 1999.
37. Soares MP, Lin Y, Anrather J, Csizmadia E, Takigami K, Sato K, Grey ST, Colvin RB, Choi AM, Poss KD, and Bach FH. Expression of heme oxygenase-1 (HO-1) can determine cardiac xenograft survival. *Nat Med* 4: 1073–1077, 1998.
38. Tassi S, Carta S, Vené R, Delfino L, Ciriolo MR, and Rubartelli A. Pathogen-induced interleukin-1beta processing and secretion is regulated by a biphasic redox response. *J Immunol* 183: 1456–1462, 2009.
39. Tojo T, Ushio-Fukai M, Yamaoka-Tojo M, Ikeda S, Patrushev N, and Alexander RW. Role of gp91phox (Nox2)-containing NAD(P)H oxidase in angiogenesis in response to hindlimb ischemia. *Circulation* 111: 2347–2355, 2005.
40. Tosetti F, Venè R, Arena G, Morini M, Minghelli S, Noonan DM, and Albini A. *N*-(4-hydroxyphenyl)retinamide inhibits retinoblastoma growth through reactive oxygen species-mediated cell death. *Mol Pharmacol* 63: 565–573, 2003.
41. Valetti C and Sitia R. The differential effects of dithiothreitol and 2-mercaptoethanol on the secretion of partially and completely assembled immunoglobulins suggest that thiol-mediated retention does not take place in or beyond the Golgi. *Mol Biol Cell* 5: 1311–1324, 1994.
42. van Anken E, Romijn EP, Maggioni C, Mezghrani A, Sitia R, Braakman I, and Heck AJ. Sequential waves of functionally related proteins are expressed when B cells prepare for antibody secretion. *Immunity* 18: 243–253, 2003.
43. Xia ZW, Zhong WW, Meyrowitz J S, and Zhang ZL. The role of heme oxygenase-1 in T cell-mediated immunity: the all encompassing enzyme. *Curr Pharm Des* 14: 454–464, 2008.
44. Zangar RC, Davydov DR, and Verma S. Mechanisms that regulate production of reactive oxygen species by cytochrome P450. *Toxicol Appl Pharmacol* 199: 316–331, 2004.

Address correspondence to:
Dr. Anna Rubartelli
Cell Biology Unit
National Cancer Research Institute
Largo Rosanna Benzi 10
Genova
Italy

E-mail: anna.rubartelli@istge.it

Date of first submission to ARS Central, December 29, 2009; date of final revised submission, March 10, 2010; date of acceptance, April 1, 2010.

Abbreviations Used

Ab = antibody
CHX = cycloheximide
DC = dendritic cell
DPI = diphenylene iodonium
GSH = glutathione
H_2DCF-DA = 2′,7′-dichlorofluorescein diacetate
H_2O_2 = hydrogen peroxide
HO-1 = heme-oxygenase-1
MCB = monochlorobimane
MFI = mean fluorescence intensity
NEM = *N*-ethylmaleimide
NPSH = nonprotein thiol
PG1 = PeroxyGreen1
ROS = reactive oxygen species
SRBC = sheep red blood cell
Trx = thioredoxin

This article has been cited by:

1. Yuhui Yang, Svetlana Karakhanova, Sabine Soltek, Jens Werner, Pavel P. Philippov, Alexandr V. Bazhin. 2012. In vivo immunoregulatory properties of the novel mitochondria-targeted antioxidant SkQ1. *Molecular Immunology* **52**:1, 19-29. [CrossRef]
2. Katie E. Crump, Daniel G. Juneau, Leslie B. Poole, Karen M. Haas, Jason M. Grayson. 2012. The reversible formation of cysteine sulfenic acid promotes B-cell activation and proliferation. *European Journal of Immunology* **42**:8, 2152-2164. [CrossRef]
3. Milena Bertolotti , Roberto Sitia , Anna Rubartelli . 2012. On the Redox Control of B Lymphocyte Differentiation and Function. *Antioxidants & Redox Signaling* **16**:10, 1139-1149. [Abstract] [Full Text HTML] [Full Text PDF] [Full Text PDF with Links]
4. Marizela Delic, Corinna Rebnegger, Franziska Wanka, Verena Puxbaum, Christina Haberhauer-Troyer, Stephan Hann, Gunda Köllensperger, Diethard Mattanovich, Brigitte Gasser. 2012. Oxidative protein folding and unfolded protein response elicit differing redox regulation in endoplasmic reticulum and cytosol of yeast. *Free Radical Biology and Medicine* **52**:9, 2000-2012. [CrossRef]
5. Maura Gasparetto, Sanja Sekulovic, Chad Brocker, Patrick Tang, Anush Zakaryan, Ping Xiang, Florian Kuchenbauer, Maggie Wen, Katayoon Kasaian, Marie France Witty, Patty Rosten, Ying Chen, Suzan Imren, Gregg Duester, David C. Thompson, Richard Keith Humphries, Vasilis Vasiliou, Clay Smith. 2012. Aldehyde dehydrogenases are regulators of hematopoietic stem cell numbers and B-cell development. *Experimental Hematology* **40**:4, 318-329.e2. [CrossRef]
6. Philippe J. Nadeau, Annie Roy, Catherine Gervais-St-Amour, Marie-Ève Marcotte, Nathalie Dussault, Sonia Néron. 2012. Modulation of CD40-activated B lymphocytes by N-acetylcysteine involves decreased phosphorylation of STAT3. *Molecular Immunology* **49**:4, 582-592. [CrossRef]
7. Roberta Venè , Patrizia Castellani , Laura Delfino , Maria Lucibello , Maria Rosa Ciriolo , Anna Rubartelli . 2011. The Cystine/Cysteine Cycle and GSH Are Independent and Crucial Antioxidant Systems in Malignant Melanoma Cells and Represent Druggable Targets. *Antioxidants & Redox Signaling* **15**:9, 2439-2453. [Abstract] [Full Text HTML] [Full Text PDF] [Full Text PDF with Links] [Supplemental material]
8. Michela Vezzoli , Patrizia Castellani , Gianfranca Corna , Alessandra Castiglioni , Lidia Bosurgi , Antonella Monno , Silvia Brunelli , Angelo A. Manfredi , Anna Rubartelli , Patrizia Rovere-Querini . 2011. High-Mobility Group Box 1 Release and Redox Regulation Accompany Regeneration and Remodeling of Skeletal Muscle. *Antioxidants & Redox Signaling* **15**:8, 2161-2174. [Abstract] [Full Text HTML] [Full Text PDF] [Full Text PDF with Links] [Supplemental material]
9. Jose Manuel Garcia-Manteiga, Silvia Mari, Markus Godejohann, Manfred Spraul, Claudia Napoli, Simone Cenci, Giovanna Musco, Roberto Sitia. 2011. Metabolomics of B to Plasma Cell Differentiation. *Journal of Proteome Research* 110729130128094. [CrossRef]
10. Emily M. Lynes, Thomas Simmen. 2011. Urban planning of the endoplasmic reticulum (ER): How diverse mechanisms segregate the many functions of the ER. *Biochimica et Biophysica Acta (BBA) - Molecular Cell Research* . [CrossRef]
11. Marcus Conrad, Hideyo Sato. 2011. The oxidative stress-inducible cystine/glutamate antiporter, system x c - : cystine supplier and beyond. *Amino Acids* . [CrossRef]
12. Éva Margittai, Roberto Sitia. 2011. Oxidative Protein Folding in the Secretory Pathway and Redox Signaling Across Compartments and Cells. *Traffic* **12**:1, 1-8. [CrossRef]
13. Milena Bertolotti , Sun Hee Yim , Jose M. Garcia-Manteiga , Silvia Masciarelli , Yoo-Jin Kim , Min-Hee Kang , Yoshihito Iuchi , Junichi Fujii , Roberta Vené , Anna Rubartelli , Sue Goo Rhee , Roberto Sitia . 2010. B- to Plasma-Cell Terminal Differentiation Entails Oxidative Stress and Profound Reshaping of the Antioxidant Responses. *Antioxidants & Redox Signaling* **13**:8, 1133-1144. [Abstract] [Full Text HTML] [Full Text PDF] [Full Text PDF with Links] [Supplemental material]